J. Bangladesh Acad. Sci., Vol. 44, No. 1, 43-52, 2020
DOI: https://doi.org/10.3329/jbas.v44i1.48562

A WET CHEMICAL SYNTHESIS AND CHARACTERIZATION OF MWCNT-STARCH BIOCOMPOSITES

NAFISA ALAM[1,2], KAZI HANIUM MARIA[2]*, MOHAMMAD JELLUR RAHMAN[3], PARVIN SULTANA[3], TETSU MIENO[4]
[2]*Department of Physics, University of Dhaka, Dhaka-1000, Bangladesh*

ABSTRACT

MWCNT/starch composites were prepared by simple solution casting method by incorporating upto 1.0 wt. % of multi-walled carbon nanotubes (MWCNTs) as reinforcing fillers in the starch matrix. Gelatin was used as dispersing agent to disperse the MWCNTs into aqueous solution and glycerol was used as plasticizer to form composites. SEM images of the MWCNT/starch composite show the homogenous surface of the composite where CNTs are embedded into the starch matrices. XRD spectra of the composite show no characteristic peaks of CNTs in the starch matrix. FTIR spectra show peaks at around 3435 and 2927 cm^{-1} indicating that the covalent bonds between –OH groups and C-H groups of soluble starch and CNT were formed in the composite. Electrical conductivity of the composite was enhanced from $2.85\times10^{-9}$to 5.28×10^{-8} S/m due to the addition of CNTs at room temperature and decreased with the increase of temperature. UV visible spectra showed increasing absorption with increasing CNTs content in the composite. TGA analysis demonstrated the stability of the MWCNT/starch composite.

Keywords: Biocomposites; MWCNTs; Starch; Gelatin; Conductivity.

INTRODUCTION

In recent years, carbon nanotubes and their composite materials have been extensively investigated for the development of renewable source-based biodegradable materials because of the worldwide environment problems resulting from the use of plastics (Maria and Mieno 2017, Rahman and Mieno, 2015). Several polymers have been explored towards the development of biodegradable materials (Alam *et al.*, 2018, Maria and Mieno 2017, Rahman and Mieno, 2015). Among them, starch is a natural biodegradable polymer and it could be used as a good alternative for biodegradable packaging applications. Starch is odorless, tasteless, colorless, nontoxic, biologically absorbable and widely available. It can be obtained from different agricultural products like cereal grains (corn, wheat, rice), seeds, legumes (lentils) and tubers (potato and cassava). Besides, its cost is relatively lower than that of other biodegradable polymers. Starch is a polymeric carbohydrate composed of a mixture of two biopolymers: amylose (straight chain) and amylopectin (branched chain) (Zeleke *et al.*, 2016). The structure of the starch granule depends on the structural distribution of amylose and amylopectin. The ratio between amylose and amylopectin varies in different starch sources. Generally, starch contains about 20-25 % of amylose and 75-80% of amylopectin. Generally, starch's mechanical properties are very poor (Zheng *et al.*, 2013). Incorporation of nanofillers such as CNTs in biopolymers is a promising route to enhance the structural, mechanical and electrical properties of biopolymers. Because of having a very high aspect ratio (i.e. length to

*Corresponding author:<kazimaria@du.ac.bd>.
[1]Nuclear Power Plant Company Bangladesh Limited, Ramna, Dhaka-1217, Bangladesh
[3]Department of Physics, Bangladesh University of Engineering and Technology, Dhaka – 1000, Bangladesh
[4]Graduate School of Science and Technology, Shizuoka University, Shizuoka 422-8529, Japan

diameter ratio) and Young's modulus, CNTs are expected to be an excellent reinforcement material to produce starch nanocomposite. Usually CNTs exist in aggregation form and make large bundles because of the strong van der Waals interactions between the sidewalls of the tubes which make CNT insoluble in aqueous solution. The applications of CNTs are obstructed by this insoluble nature of CNTs. Assembled CNTs easily clot in polymer matrix and weaken the reinforcing effects. But amylose of starch can form single helix in homogeneous CNT solutions by hydrophobic interactions (Fu *et al.* 2007, Star *et al*. 2002). In our previous study, we developed a convenient method to disperse CNT in water by using gelatin (Maria and Mieno 2016). Water-soluble gelatin is composed of different types of amino acid chains which may wrap around the sidewalls of the CNTs through a hydrophobic-hydrophobic interaction (Chang *et al.,* 2011). The wrapping mechanism of polymer is believed to eliminate hydrophobic interface between the nanotubes and the aqueous medium. Gelatin has a zwitterionic structure and its amino acid shows the hydrophobic nature. The interaction between the hydrophobic amino acids and the hydrophobic wall of the CNTs might modify the CNTs by including a hydrophilic group and disperse them in water (Maria and Mieno 2017). Moreover, gelatin does not affect the physical properties of CNTs. Uniformly dispersed CNTs in the aqueous solution may form strong interactions between starch and CNTs to improve the mechanical properties, electrical properties and water vapor resistance of the carbon nanotube starch composite (Maria and Mieno 2017).The objective of this work is to prepare starch/CNT composites by incorporating different amounts of MWCNTs in starch which might have a great importance for potential applications as high-performance biodegradable materials. The synthesized MWCNT/starch composites are expected to have some superior mechanical, electrical and thermal properties. However, not much study is reported about the starch/CNT composites (Fama *et al.,* 2011, Zheng *et al.*, 2013, Cheng *et al.,* 2013, Chang *et al.* 2011). In this investigation, MWCNT/starch composite film was prepared by solution casting method. Here, gelatin was used to disperse CNT before mixing with starch and glycerol. Glycerol was used as plasticizer to make the composite stable. Our objective was to obtain a low cost composite with good environmental stability by a facile method. The resulting starch/CNT composite shows high electrical conductivity and thermal stability. The composite properties could be improved by increasing the amount of CNTs and a product of any size and shape could be obtained by maintaining the MWCNT/starch ratio. The properties of the composites are reported in this article.

MATERIALS AND METHODS

MWCNTs (Sigma-Aldrich, outer diameter= 10–30 nm, inner diameter 3–10 nm, length 1–10 μm, and purity>90%), gelatin (Wako 1st Grade, appearance: yellowish brown and crystalline powder), starch soluble (Qualikems, loss on drying at 105°C 10%, sulfated ash=0.5%, chloride = 0.04%), and glycerol (Emplura) were purchased and used as received. At first, 5 mg MWCNTs were added to 20 mL distilled water in a beaker. 30 mg gelatin was added to the mixture to disperse MWCNTS with the water. Then the mixture was sonicated in an ultra-sonication bath for about two hours to get a homogenized solution. 2.5 g starch and 0.3 mL glycerol were added to the homogenized solution. The mixture was heated up to 90 ˚C until complete gelatinization. Stirring was continued during gelatinization process by a magnetic stirrer. The resulting gel was

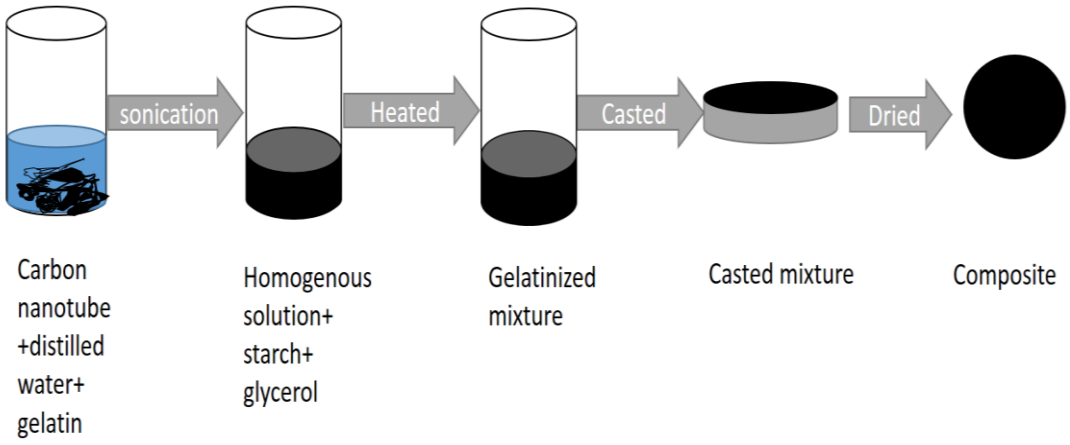

Fig. 1. Schematic diagram of preparation of MWCNT/starch composite

subsequently cast in glass petri dishes. Then the gel was dried for an hour in an oven at 120˚C and then at room temperature for 24 hours. The obtained sheets were preserved in an airtight bag, ready for characterizations. Figure 1 shows the complete procedure for synthesizing of CNT/starch composites.

MWCNT/starch composite with different wt.% of MWCNTs were prepared to investigate their different properties. The surface morphology and structural behavior were studied by Scanning Electron Microscope (SEM, JEOL JSM-7600F, USA) and X-ray diffraction (XRD, Rigaku Smart Lab) with filter for CuK_{α} irradiation at λ = 1.5406 Å. FTIR spectra were obtained using Shimadzu IR Prestige-21 to confirm the presence of various functional groups in the composite. DC electrical conductivity was measured by placing the sample between two copper electrodes using pressure contacts (Fig. 2). The current across the sample was measured by using an electrometer where dc voltage was applied from a power supply. UV visible absorption was measured at room temperature in the range of 300–1200 nm with a Cary 5000-Scan UV–vis–NIR spectrophotometer.

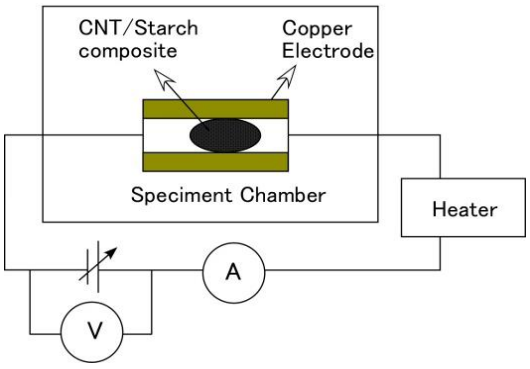

Fig. 2. Schematic diagram of experimental set up of electrical measurement

RESULTS AND DISCUSSION

Fig. 3 shows XRD spectra of starch, MWCNTs, starch sheet and CNT/starch composite with two different concentrations. The XRD pattern of starch powder exhibits the pattern of a crystalline material and shows the strongest peak at 17.24^0. The peak at 15.34^0 has been converted into a shoulder like signal and a couple of weak

peaks scattered around 23.36^0 and 24^0. The occurrence of these peaks confirms that the starch used in our study belongs to 'A' pattern (Zeleke *et al.*, 2016). Typical XRD pattern of MWCNTs indicates a crystalline structure. The strongest diffraction peak at the angle of 25.9^0 can be indexed as the C (002) reflection because of the hexagonal graphite structure. The other characteristic diffraction peak of graphite at 43^0 can be associated with C (100) (Lu *et al.*, 2008; Rosca *et al.*, 2005). Crystallinity is not expected in glycerol plasticized starch sheet. In case of the starch sheet, powder starch was completely gelatinized in the presence of water and glycerol.

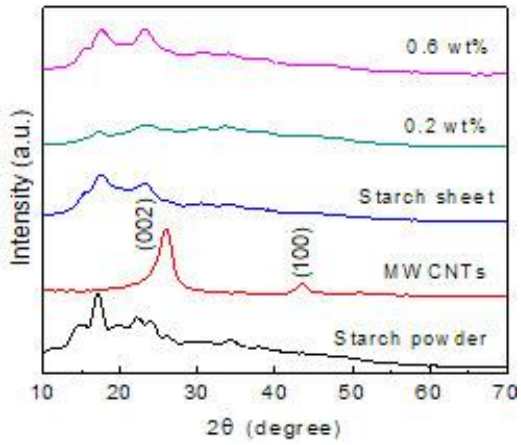

Fig. 3. XRD graphs of starch, MWCNTs, pure starch sheet and MWCNT/starch sheet with different amount of CNTs (0.2 and 0.6 wt. %)

Glycerol and water molecules cause exchange of starch intermolecular and intramolecular hydrogen bonds which may reduce the crystallinity of starch by entering into starch granules. Therefore the crystalline transformation from A- to V- type was expected to be observed in the XRD pattern of the starch sheet. However, V-type starch crystallinity is not observed in the XRD pattern of starch sheet. It may be owing to spontaneous recrystallization of starch molecules after gelatinization (Wang *et al.*, 2008). The XRD spectra of CNT/starch composite show crystalline structure with peaks around 17.2^0 and 23.1^0. No peak associated with CNTs is observed in the XRD spectra of CNT/starch composites which indicate uniform dispersion of MWCNTs in the composite. The sharpness and intensity of peaks increased with MWCNTs concentration and this sharpness clearly points out interactions between MWCNTs and starch (Lee *et al.*, 2014).

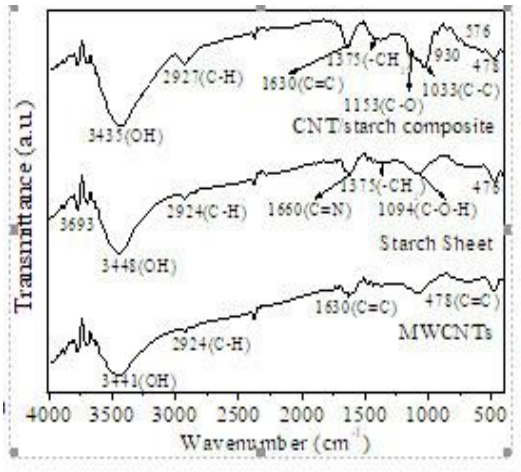

Fig. 4. FTIR spectra of CNT/starch composite with 1 wt. % MWCNTs load, starch sheet and MWCNTs

Fig. 4 shows the FTIR spectra of pure MWCNTs, pure starch and CNT/starch composite. The absorption regions are marked at 3440, 1630 cm^{-1} which could be associated with the adsorbed water on CNT. The broad absorption peak at 3440 cm^{-1} may be attributed to O-H stretching vibration of the adsorbed water on CNT. The absorptions at 1630 cm^{-1} may be attributed to water adsorbed on CNT or C=C stretching vibration of CNT (Cheng et. al., 2013). The absorption peak at 478 cm^{-1} may be attributed to C=C bending vibration. In case of pure starch composite, the absorption regions are observed at 3448 and 1625 cm^{-1} which may be

ascribed to water molecules (Iizuka and Aishima 1999). It is found that the absorption peak of pure starch at 3448 cm^{-1} is broader than the absorption peak of MWCNTs. Infrared band with a peak at 1637 cm^{-1} identifies water adsorption in the amorphous region of starch (Kizil *et. al.,* 2002). The FTIR spectrum of starch shows a peak at 2924 cm^{-1} which may be due to the C-H stretching vibration of methylene groups (Zheng *et al.,* 2013). The bending and deformation vibrational bands related to the carbon and hydrogen atoms are supposed to be observed in the region 1500-1300 cm^{-1} (Kizil *et al.,* 2002). The peak at 1375 cm^{-1} may be ascribed to bending modes of O-C-H, C-C-H, and C-O-H angles (Iizuka and Aishima 1999). The infrared band at the 1344 cm^{-1} may have originated from CH_2 bending modes (Kizil *et al.,* 2002). The peak at 1094 cm^{-1} is attributed to C-O bond stretching of the C-O-C group or C-O-H bending modes (Zheng *et al.,* 2013, Kizil *et al.,* 2002). Here the bands at 581 cm^{-1} and 476 cm^{-1} may be attributed to the skeletal modes of the pyranose ring. FTIR spectra of CNT/starch composite shows much broader peak at 3435 cm^{1} which is due to O-H stretching vibration. Both pure starch and MWCNT/starch composite show broad peaks around 3440 cm^{-1} which indicate the absorption of water due to the presence of glycerol (Kizil *et al.,* 2002). The peak at 2927 cm^{-1} indicates the N-H stretching vibration or hydrogen bonded salt of amino acid due to the presence of gelatin. The peak at 1630 cm^{-1} may be attributed to the (O-H) bending of water present in the starch or C=C stretching vibration. The presence of starch component is confirmed by the absorption peak at 1375 cm^{-1}. The peak at 1153 cm^{-1} is ascribed to the coupling modes of C-O and C-C stretching (Chang *et al.,* 2011). The peak at 1080 cm^{-1} is ascribed to C-O bond stretching of the C-O-C group. Thus it is demonstrated that CNTs are present in starch composite (Zheng *et al.,* 2013). The infrared absorption band at 930 cm^{-1} is ascribed to the glycosidic linkages in starches (Chang *et al.,* 2011). Infrared spectra exhibit complex vibrational modes at low wavenumbers due to the skeletal mode vibrations of the glucose pyranose ring. Bands at 576 cm^{-1} and 478 cm^{-1} in the infrared spectra may be attributed to the skeletal modes of the pyranose ring (Kizil *et al.,* 2002). These characteristic peaks demonstrate that strong covalent bonds may form between –OH groups of soluble starch and CNT. A summary of the functional groups assignment of starch, MWCNTs and CNT/starch composite based on IR spectra is given in Table 1.

Table 1. Assignment of functional groups of starch, MWCNTs and CNT/starch composite based on IR spectra

Frequency range (cm^{-1})	**Functional groups assignment & vibration type**	**compounds**
≈ 3448, ≈3441, ≈3435	-OH stretching	Starch, MWCNT, CNT/starch composite
≈ 2924, ≈2927	C-H stretching	Starch, MWCNT, CNT/starch composite
≈ 1630	C=C stretching	MWCNT, CNT/starch composite
≈ 1375	-CH_2 bending	Starch, CNT/starch composite
≈ 1153	C-O stretching	CNT/starch composite
≈ 1094	C-O-H bending	Starch
≈ 1033	C-C stretching	CNT/starch composite
≈ 478	C=C bending	MWCNT, CNT/starch composite

The SEM micrographs of CNT/starch composites of different wt. % of CNTs at different magnification taken to study the surface morphology of the composites are shown in Fig. 5. As no MWCNTs are clearly seen in SEM micrographs, it can be claimed that MWCNT disperses well in the starch matrix. It is conjectured that MWCNTs is wrapped by the starch matrix due to the strong interaction between starch and MWCNTs (Maria and Mieno, 2016). In the case of 0.6 wt. % loading, CNTs are not clearly shown in the image (Fig. 5(a)). But with the high loading like 0.8 wt. % and 1 wt. %, edge of CNTs is observed on the surface of the composite (Fig. 5 (b) and (c)). At 1 wt. % loading (Fig. 5(d)), MWCNTs are observed to be agglomerated into clusters because of the failure of MWCNT-starch adhesion (Fama *et al*., 2011).

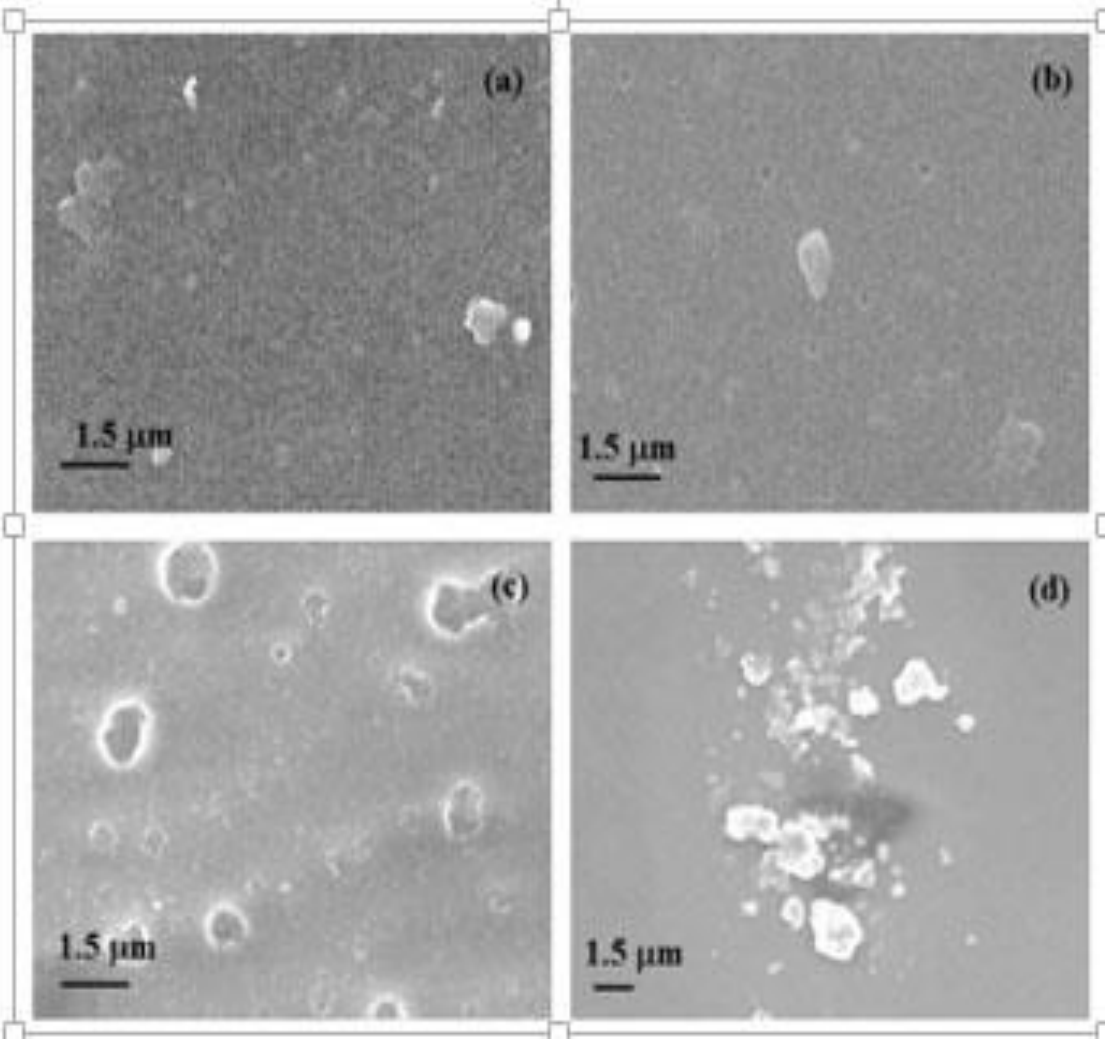

Fig. 5. SEM micrographs of (a) 0.6 wt. % , (b) 0.8 wt. % (c) 1 wt. % CNT/starch composite at 10k and (d) 1 wt. % CNT/starch composite at 5k magnification

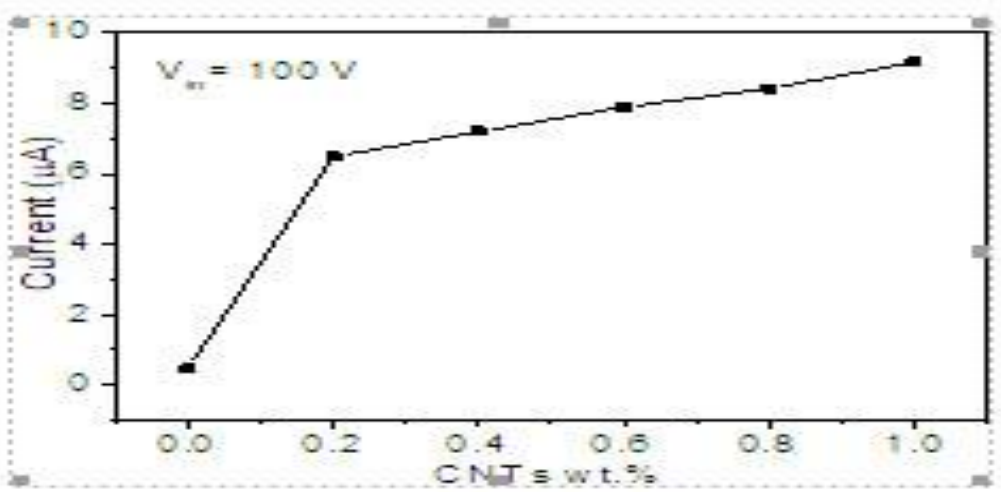

Fig. 6. Variation of Current and amount of MWCNTs in MWCNT/starch composite at room temperature where the input voltage *V*in = 100V.

In order to determine the effect of MWCNTs loading on the conductivity of the composite, dc electrical measurement was carried out. Fig. 6 shows the variation of Current with the loading of MWCNT in the composite at room temperature and applied voltage of 100V. It is clearly seen from Fig. 6 that current increases with the increase of MWCNTs content. Temperature variation of conductivity was measured by using a heating coil wrapped around the specimen chamber. Temperature dependence of the measured current as function of applied voltage at various temperatures is shown in Figs. 7(a) and 7(b) for pure starch and starch 1% MWCNT composite respectively. It is clear that the I-V variation is not Ohmic, and that conductivity decreases with increase in temperature as is expected for metallic conduction. The conductivity was evaluated from the observed current at an applied voltage of 100 V. Fig. 8 shows the conductivity of pure starch and the composites of various compositions at various temperatures.

Though starch is an insulating material, a small current is observed in the case of pure starch sheet which also decreases with increase in temperature. Incorporation of 1 wt % of MWCNTs in starch brings about more than 10-fold increase in the observed current (Fig. 6). This increase may be attributed to the creation of a nanotube network for electron transfer between the electrodes through the composite. Figure 6 shows that conductivity increases with increasing amount of MWCNTs in composite. The conductivity increased from 2.85×10^{-9} S/m for pure starch sheet to 5.28×10^{-8} S/m for the CNT/starch composite with 1 wt. % MWCNTs loading at room temperature. With higher MWCNT content, the nanotube network expands offering more channels for transport of electrons and thus facilitating electrical conduction.

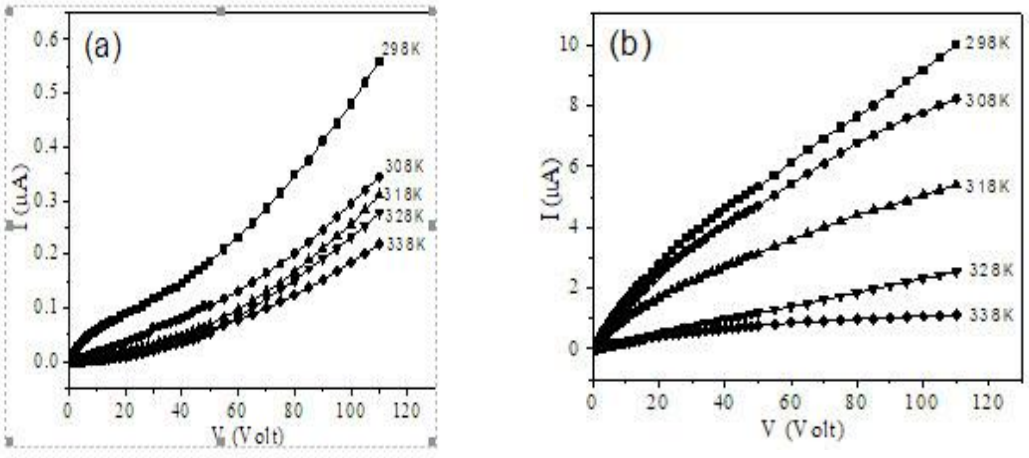

Fig. 7. I-V characteristics curve for **(a)** pure starch sheet **(b)** 1 wt % CNT/starch composite at different temperature.

TGA analysis of starch sheet, MWCNT/starch composite and starch powder was carried out from room temperature to 600^{0}C. Fig. 9 shows that the thermal degradation occurs in two different steps in between 250-320^{0}C. The mass loss of starch powder is almost 20% less than starch sheet and MWCNT/starch composite, which may be because of volatilization of water and glycerol present in starch sheet and CNT/starch composite. The mass loss of both starch sheet and MWCNT/starch composite is almost 50% in thermal degradation range. The final degradation of MWCNT/starch composite is 3% less than starch sheet. Consequently, it can be inferred that incorporation of MWCNT increases thermal stability of the MWCNT/starch composite. Further work will be carried out by using higher wt. % of MWCNTs in the starch matrix for improving the stability of the composite.

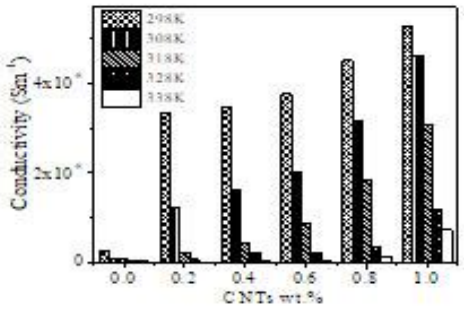

Fig. 8. Conductivity vswt. % of CNTs in MWCNT/starch composite graph with increasing temperature

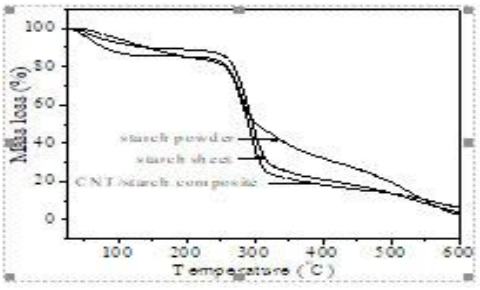

Fig.9. TGA graph of starch sheet, MWCNT/starch composite and starch powder.

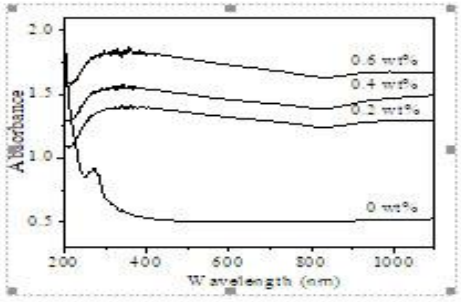

Fig.10. UV−visible spectra of MWCNT/starch composite with the increasing concentrations of MWCNTs from the bottom to top.

Fig. 10 shows the UV visible spectra of pure starch sheet and MWCNT/starch composites with different amount of MWCNTs. The absorbance of the composites increases significantly due to addition of MWCNTs in starch. Further with increase in concentration of MWCNTs in the composite the absorbance also increases. Thus, MWCNT/starch composites can be used as UV absorber to mitigate the damaging effect of UV lights (Soet *et al.*, 1996).

CONCLUSION

MWCNT/starch composites were successfully prepared. It has been shown that they possess higher electrical conductivity, improved thermal stability and UV absorption compared to pure starch sheets. Controlled incorporation of MWCNTs in the composite is expected to pave the way for a much broader range of applications of the composites. The prepared MWCNT/starch composite could be used as electroactive polymer, biosensors, electronic device, orthopedic applications, and artificial arms in robotics, UV shielding, gas and flame protection and alternative of petroleum based packaging.

REFERENCES

Alam KMM, Beg MDH, Yunus RM, Bijarimi, M. Mina MF, Maria KH and Mieno T, 2018. Modification of structure and properties of well-dispersed dendrimer coated multi-walled carbon nanotube reinforced polyester nanocomposites. *Polymer test.* **68**: 116-125.

Chang PR, Zheng P, Liu B, Anderson DP, Yu J and Ma X. 2011. Characterization of magnetic soluble starch-functionalized carbon nanotubes and its application for the adsorption of the dyes. *J. Hazard. Mater* **186**: 2144–2150.

Cheng J, Zheng P, Zhao F, and Ma X. 2013. The composites based on plasticized starch and carbon nanotubes. *Int. J. Biol. Macromol* **59**: 13-19.

Fama LM, Pettarin V, Goyanes SN and Bernal CR, 2011. Starch/multi-walled carbon nanotubes composites with improved mechanical properties. *Carbohydrate Polymers* **83**: 1226-1231.

Fu C, Meng L, Lu Q, Zhang X and Gao C. 2007. Large-scale production of homogeneous helical amylose/SWNTs complexes with good biocompatibility. *Macromol. Rapid Commun*. **28**: 2180-2184.

Iizuka K. and Aishima T. 1999. Starch Gelation Process Observed by FT-IR/ATR Spectrometry with Multivariate Data Analysis. *J. Food Science* **64**:653-658.

Kizil R, Irudayaraj J and Seetharaman K.. 2002. Characterization of Irradiated Starches by Using FT-Raman and FTIR Spectroscopy. *J. Agri Food Chem* **50:** 3912−3918.

Lee JH, Kim MT, Rhee KY and Park SJ. 2014. An experimental investigation on the conductive behavior of carbon nanotube-reinforced natural polymer nanocomposites. *Res. Chem. Intermed* **40**: 2487–2493.

Lu C, Su F and Hu S. 2008. Surface modification of carbon nanotubes for enhancing BTEX adsorption from aqueous solutions. *Applied Surface Science* **254**: 7035-7041.

Ma X, Yu J and Wang N. 2008. Glycerol plasticized-starch/multiwall carbon nanotube composites for electroactive polymers. *Composites Science and Technology* **68**: 268-273.

Maria KH and Mieno T. 2016. Effect of gelatin on the water dispersion and centrifugal purification of single-walled carbon nanotubes. *Jpn. J. Appl. Phy* **55**: 01AE04.

Maria KH and Mieno T. 2017. Production and properties of carbon nanotube/cellulose composite paper. *J. Nanomaterials* **2017**: 6745029.

Maria KH and Mieno T. 2018. Production of Water Dispersible Carbon Nanotubes and Nanotube/Cellulose Composite-*Carbon Nanotubes - Recent Progress* Intech open. pp. 235-259.

Rahman MJ and Mieno T. 2015. Conductive cotton textile from safely functionalized carbon nanotubes. *J. Nanomaterials* **2015**: 978484.

Rosca ID, Watari F, Uo M and Akasaka T. 2005. Oxidation of multiwalled carbon nanotubes by nitric acid. *Carbon* **43**: 3124-3131.

Soest JJGV, Hulleman SHD, Wit DD and Vliegenthart JFG. 1996. Crystallinity in starch bioplastics. *Ind. Crop Prod.* **5**:11-22.

Star A, Steuerman DW, Heath JR and Stoddart JF. 2002. Starched carbon nanotubes. *Angewandte Chemie International Edition* **41**: 2508-2512.

Zeleke TD, Segne TA and Chebude Y. 2016. Synthesis and Characterization of Starch Vernolates in Organic Solvents. *American J Appl. Chemistry* **4**: 212-220.

Zheng P, Ma T and Ma X. 2013. Fabrication and Properties of Starch-Grafted Graphene Nanosheet / Plasticized-Starch Composites. *Ind. Eng. Chem. Res.* **52**: 14201-14207.

(Received 27 February 2020; revised 3 May 2020, accepted May 15, 2020)